Taylor & Francis
Taylor & Francis Group

ELECTROANALYTICAL

Electrochemical Behavior of Verapamil at Graphite–Polyurethane Composite Electrodes: Determination of Release Profiles in Pharmaceutical Samples

Felipe S. Semaan,[1,2] Éder T. G. Cavalheiro,[1]
and Christopher M. A. Brett[2]

[1]Instituto de Química de São Carlos, University of São Paulo,
São Carlos, Brazil
[2]Departamento de Química, Faculdade de Ciências e Tecnologia,
University of Coimbra, Coimbra, Portugal

Abstract: A solid graphite–polyurethane composite electrode has been used to determine release profiles of verapamil, a calcium-channel blocker. The electro-oxidation process was characterized by cyclic voltammetry and electrochemical impedance spectroscopy and showed no adsorption of analyte or oxidation products, unlike at other carbon-based electrodes. Quantification gave linear ranges up to $40\,\mu mol\,L^{-1}$ with cyclic voltammetry and detection limits of $0.7\,\mu mol\,L^{-1}$ by differential pulse and square-wave voltammetry. Commercial product samples were successfully analyzed with results equal to those from spectrophotometry. Because no electrode surface renewal is needed, this electrode material has many advantages.

Keywords: Composite electrode, release profile, verapamil

INTRODUCTION

In recent decades, a wide group of drugs for controlling blood pressure has been developed and studied. The first group was the diuretics, followed by the beta-blockers and calcium-channel blockers. In 1964, propanolol started to be sold as Inderal, the first commercially available beta-blocker. Its success triggered a quest for similar drugs and led to the development of verapamil (Patlak 2003). Considered the first calcium-channel blocker, verapamil is widely used in its hydrochloride form and is a synthetic drug derived from papaverin, a phenylalkylamine, with important applications in *Angina pectoris* and hypertension (Beevers, Lip, and O'Brien 2007; Moser 2008; Jhee et al. 2005). Its structural formula is presented in Fig. 1 ($C_{27}H_{38}N_2O_4 \cdot HCl$, $pK_a = 8.7$) (Ramírez-Campos and Villafuertes-Robles 2004). This drug exists as R and S isomers, with different biological efficiencies, which does not occur with other drugs in the same category (Borges et al. 2005).

Verapamil has been determined in various matrices such as in pharmaceutical products and biological samples using different methods of detection, as briefly described here and summarized in Table 1. Such procedures include analysis in the ultraviolet-visible (UV-vis) region after derivatization (Rahman and Hoda 2002; Rahman and Azmi 2004), UV-vis spectrophotometry after chromatographic separation (Gil-Agustí et al. 2006; Venkatesh et al. 2007), fluorometry (Silva et al. 2002), chromatographic procedures (Jhee et al. 2005; Borges et al. 2005; Rambla-Alegre et al. 2005; Li et al. 2007), resonance Rayleigh scattering coupled to a flow-injection system (Xu et al. 2007), positive electron-spray ionization (Walles et al. 2002), and capillary electrophoresis (Kristoffersen et al. 2007; Capella-Peiró et al. 2007).

Electroanalytical procedures have been also reported. Hassan et al. (1999) presented a miniaturized solid-state potentiometric sensor based on carboxylated polyvinyl chloride (PVC) and Nafion, reaching Nernstian response between 10^{-2} and 10^{-5} mol L^{-1}. Polymeric electrodes
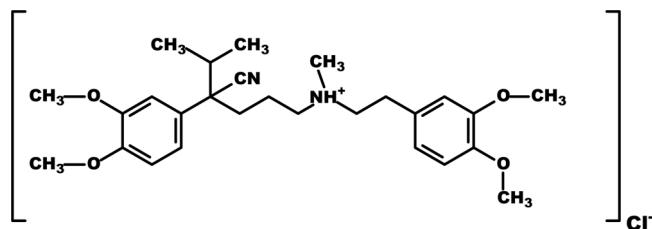

Figure 1. Structural formula of verapamil hydrochloride.

Table 1. Analytical parameters in the literature for the determination of verapamil by different techniques

Technique	Limit of detection (μmol L^{-1})	Linear range (μmol L^{-1})	Reference
Spectrophotometry	—	0–690	Rahman and Azmi 2004
Spectrophotometry	—	20.4–407	Gil-Agustí et al. 2006
HPLC-UV	0.3	0.2–0.95	Venkatesh et al. 2007
HPLC-UV	6.7	22–220	Silva et al. 2002
Fluorimetry	0.082	—	Rambla-Alegre et al. 2005
Rayleigh scattering	0.01	0.04–26.5	Walles et al. 2005
HPLC-MS-MS	0.02	0.02–5.06	Ramírez-Campos and Villafuertes-Robles 2004
HPLC-MS-MS	—	0.002–1.10	Rahman and Hoda 2002
HPLC-MS	5.0×10^{-4}	0.01–1.00	Kristoffersen et al. 2007
HPLC-MS-MS	—	4.07–815	Xu et al. 2007
HPLC-MS	0.005	—	Capella-Peiró et al. 2007
Capillary electrophoresis	0.077	1.10–44.0	Hassan et al. 1999
Potentiometry	—	10–10000	Ortuño, Sánchez-Pedreño, and Gil 2005
Potentiometry	—	5.0–100.0	Ortuño, Hernández, and Sánchez-Pedreño 2006
Potentiometry	—	10–10000	Aboukasim et al. 2002
Voltammetry	0.13	0.8–100	Demircan, Kir, and Ozkan 2007

based on plasticized membranes (PVC with tetraphenylpyridinium tetraphenylborate) were developed by Ortuño, Sánchez-Pedreño, and Gil (2005), which coupled the sensor to a flow system with amperometric detection. Another potentiometric electrode based on PVC, with 2-nitrophenyl octyl ether doped with tetrabutylammonium tetraphenylborate, was also presented by Ortuño, Hernández, and Sánchez-Pedreño (2006); the linear range was from 10^{-5} to 10^{-2} mol L^{-1}.

Aboukasim et al. (2002) determined verapamil in urine and pharmaceuticals by adsorptive stripping voltammetry at a mercury electrode. Demircan, Kir, and Ozkan (2007) analyzed verapamil in pharmaceuticals and urine at a glassy carbon electrode.

Despite the large number of analytical strategies, no application to the determination of release profiles of sustained tablets was found. To optimize the rate of drug intake, thereby reducing side effects and risk of overdose, different ways of controlling the rate of drug release have been developed (Karsa and Stephenson 1994; Marvola et al. 1991; Hsieh 1993). Among these, the use of polymeric matrices and special coatings

should be highlighted (Marvola et al. 1991). For laboratory evaluation, various dissolution procedures have been described, depending not only on the pharmaceutical dosage form to be evaluated but also on the physical and chemical properties of the drug. Examples are buffers such as phosphate, acetate, citrate, simulated gastric and intestinal fluids, surfactant solutions, acidic and alkaline solutions (such as HCl and NaOH), and even water (Azarmi, Roa, and Löbenberg 2007; Donauer and Löbenberg 2007).

The use of composite electrodes based on castor oil polyurethane as the insulating phase began in 2002, when composition, proportions, potential window, and pH range of application were assessed (Mendes, Claro-Neto, and Cavalheiro 2002). This was followed by applications such as the determination of dopamine in synthetic cerebrospinal fluid in Britton–Robinson buffer, pH 7.4 (Toledo et al. 2005); imipramine using Britton–Robinson buffer, pH 7.0 (Toledo et al. 2006); hydroquinone in photographic developers using acetate buffer, pH 4.5 (Mendes, Cervini, and Cavalheiro 2006); indole-3 acetic acid in soil using H_3PO_4 solution, pH 1.6 (Toledo and Vaz 2007); and atenolol in commercial samples using universal buffer, pH 10.0 (Cervini, Ramos, and Cavalheiro 2007). In all cases, the electrode was used without modification or special preparation, showing its robustness and applicability over a wide range of pH values and samples/matrices. A chemically modified polyurethane composite electrode was used as support for an oxovanadium–salen thin film for the determination of L-dopa in a flow-injection system (Teixeira et al. 2007).

The objective of this article was to develop a new electroanalytical procedure for the determination of verapamil at graphite–polyurethane composite electrodes, without the complications of adsorption, and to apply the procedure to follow the release profiles from sustainable tablets.

EXPERIMENTAL

Reagents and Solutions

Verapamil hydrochloride was obtained from Natural Pharma (Brazil) and characterized by differential scanning calorimetry (DSC Q10, TA Instruments), infrared (IR) spectroscopy (in KBr pellets using a Nicolet 5SXC Fourier transform–IR spectrophotometer), elemental analysis (C, H, and N contents was measured using a Fisons EA 1108 CNHS-O instrument), and UV spectrophotometry (Specord S100 Carl Zeiss). According to the results, verapamil hydrochloride from Natural Pharma (Brazil) could be used as received without further purification.

Table 2. Composition of buffer solutions

Composition	pH
HCl + KCl	1.2
HCl + KCl	2.0
HOAc + NaOAc	3.3
HOAc + NaOAc	4.0
HOAc + NaOAc	5.3
$Na_2HPO_4 + NaH_2PO_4$	5.8
$Na_2HPO_4 + NaH_2PO_4$	6.9
$Na_2HPO_4 + NaH_2PO_4$	8.0
$Na_2B_4O_7 \cdot 10H_2O + NaOH$	9.3
NaOH + KCl	12.2
NaOH + KCl	13.0

A $0.0100 \, mol \, L^{-1}$ stock solution was prepared by direct dissolution of verapamil in water and was stored at room temperature ($25 \pm 1°C$) for up to 1 week. Solutions of H_2SO_4 (0.50 and $0.10 \, mol \, L^{-1}$) and buffer supporting electrolytes of $0.10 \, mol \, L^{-1}$ concentration were prepared; see Table 2. Millipore Milli-Q ultrapure water was used in the preparation of all solutions, and experiments were all carried out at room temperature.

Sample Dissolution

The commercial samples consisted of Dilacoron 120-mg Retard (Abbott) tablets, for which there is no dependence between pH and release rate, according to the manufacturer. Moreover, verapamil presents good stability in water, so it was the chosen medium for dissolution and sample handling.

Dissolution and release tests were performed by dissolving an entire tablet in 500 mL of water, with constant slight stirring at room temperature; the tablet was kept suspended in a homemade open plastic holder to avoid the disruption of the tablet coating by stirring. Aliquots of 1.0 mL were taken at intervals of 1 h, up to 6 h.

Electrode Material and Preparation

The composite electrodes were prepared as described elsewhere (Mendes, Claro-Neto, and Cavalheiro 2002). Thus, castor oil polyurethane resin was prepared by mixing 0.85 parts of prepolymer A-249 and 1.0 part

of polyol B-471 (Poliquil, Brazil). Suitable amounts of graphite powder, 1–2 μm in diameter (Aldrich, USA) were added to reach 60% in mass. This mixture was homogenized in a glass mortar for 15 min and then extruded as rods, which were left to cure for 24 h and then cut into 1-cm sections. Contacts were made using silver epoxy glue and copper wire, and the assembly was sealed in nonconducting resin. The surfaces were polished using abrasive paper followed by α-Al$_2$O$_3$ particles 1.0 μm in diameter (Arotec, Brazil). The geometric area of the composite electrode was 0.071 cm^2 (0.30 cm in diameter).

The effective active surface area was estimated by cyclic voltammetry, using 5.0 mmol L^{-1} hexacyanoferrate(II) in 0.50 mol L^{-1} KCl and different potential scan rates (10–75 mV s^{-1}). After measuring the oxidation peak current at each scan rate, Eq. (1) was used to estimate the electroactive area (Brett and Oliveira-Brett 1993):

$$I_{pa}(A) = 2.95 \times 10^5 n^{3/2} A D^{1/2} c_\infty \nu^{1/2} \tag{1}$$

in which n is number of electrons involved in the oxidation, A is the electroactive area (cm^2), D is the diffusion coefficient of hexacyanoferrate(II) in cm^2 s^{-1} (7.7×10^{-6} cm^2 s^{-1} in 0.5 mol L^{-1} KCl (von Stackelberg, Pilgram, and Toome 1953), c_∞ the bulk concentration of hexacyanoferrate(II) in mol cm^{-3}, and ν the potential scan rate in V s^{-1}. From a plot of peak current vs. scan rate, the electroactive area was found to be ~0.045 cm^2, which is 64% of the total geometric area.

Electroanalytical Procedures

A three-electrode cell with 15.0 mL of supporting electrolyte was used. The working electrode consisted of a graphite–polyurethane composite electrode, prepared as described; the reference and counterelectrodes were saturated calomel (SCE) and platinum foil (1.0 cm^2), respectively.

Voltammetric measurements were carried out using a μ-Autolab, controlled by GPES 4.9 software (Eco-Chemie, the Netherlands). The conditions of analysis were changed depending on the experiment. All experiments were performed at room temperature.

Electrochemical impedance measurements were carried out in the same electrochemical cell with a PC-controlled Solartron 1250 frequency response analyzer coupled to a Solartron 1286 electrochemical interface using ZPlot 2.4 software (Solartron Analytical, UK); frequency scans were from 65,000 Hz to 0.1 Hz with 10 measurements per frequency decade, using a sinusoidal voltage perturbation of 10 mV rms.

Spectrophotometric Method for Comparison

A spectrophotometric procedure was used as a comparative method with those results found by electroanalytical techniques. The absorbance of verapamil solutions was measured from 200 to 400 nm using a Specord S 100 Carl Zeiss spectrophotometer. Peaks at 228 and 278 nm were used to obtain the analytical curves:

$$228 \text{ nm: Abs} = 12711 \times [\text{VPM}] + 0.004, \quad R = 0.999, \; n = 5 \quad (2)$$

$$278 \text{ nm: Abs} = 4970.5 \times [\text{VPM}] + 0.001, \quad R = 0.998, \; n = 5 \quad (3)$$

Linear responses were up to 10^{-4} mol L^{-1}, and the limit of detection was 3.3×10^{-6} mol L^{-1} for both wavelengths.

RESULTS AND DISCUSSION

Cyclic Voltammetry

The electrochemical behavior of verapamil (hydrochloride) was investigated by cyclic voltammetry in the potential range from 0.0 to +1.2 V vs. SCE, at a scan rate of 10 mV s^{-1} using 7×10^{-5} mol L^{-1} verapamil in the different supporting electrolytes. Following this, a narrower potential interval from +0.5 to +1.1 V vs. SCE was used. Irreversible oxidation peaks were observed. No differences were found by changing the initial scan direction or performing deaeration.

At low pH values in sulfuric acid solutions, only a poorly defined shoulder was seen at large positive values of potential. At pH 3.3 in acetate buffer solution, a better defined peak appeared at +1.035 V vs. SCE. This peak was observed at a less negative potential with increase in pH. In acetate buffer solution at pH 5.3, a well-defined anodic peak, now at +0.883 V (of the same height as at pH 3.3), was seen, and a poorly defined shoulder at more positive potentials also appeared.

In phosphate buffer solution, pH 7.0, and at pH 8.1, the shoulder became better defined, and in the latter case a separate peak became evident at +0.699 V. Thus, in pH 9.3 Na$_2$B$_4$O$_7$ solution, two well-defined peaks were observed, the first at +0.577 V with a higher value of peak current. However, at higher pH values, verapamil solutions were slightly turbid because the neutral form was less soluble than the acidic form (pK_a = 8.7). Our results were in agreement with those of Demircan, Kir, and Ozkan (2007): at values above pH 9.0, the peak potentials did not shift with pH, which means that there are no proton-transfer steps
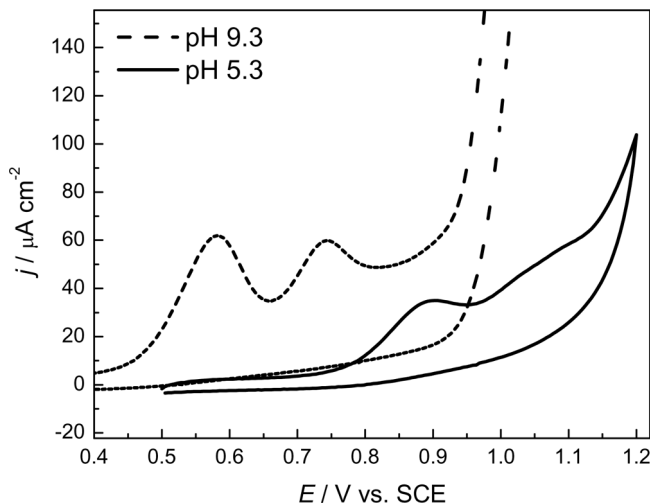
Figure 2. Cyclic voltammograms of verapamil ($6.6 \times 10^{-5}\,\mathrm{mol\,L^{-1}}$) in buffer electrolyte at pH 5.3 and 9.3 at a scan rate of $10\,\mathrm{mV\,s^{-1}}$.

associated with the electron-transfer rate-determining step (data not shown). Illustrative cyclic voltammograms of verapamil at pH 5.3 and 9.3 are shown in Fig. 2.

In all cases, the anodic peak potential moved to less positive values when pH was increased. With the exception of pH 9.25, which exhibited the greatest peak current, all the peak currents obtained in the other media had approximately the same value. From pH 3 to 9, a linear relationship between pH and the anodic peak potential was observed (Fig. 3). The slope of the plot of E_p vs. pH of 70 mV per pH unit suggests the involvement of equal number of electrons and protons.

Analysis of the second oxidation peak in the pH range 3.3–9.3 gave a slope of 60 mV per pH unit, showing that the second oxidation step also involves equal numbers of electrons and protons.

Cyclic voltammograms were recorded at different scan rates (10, 25, 50, and $100\,\mathrm{mV\,s^{-1}}$) for successive cycles in both blank and verapamil-containing solutions. The peak currents decrease after each cycle, becoming stable after five cycles. At pH 5.3, the signal became stable after the second cycle, which is unusual. In alkaline media, no signal was observed after two cycles. Further studies were therefore carried out in acetate buffer electrolyte at pH 5.3.

The influence of potential scan rate on the peak current in 7×10^{-5} mol L^{-1} verapamil solutions was measured at pH 5.3. A linear relationship with the square root of scan rate obeyed the relation
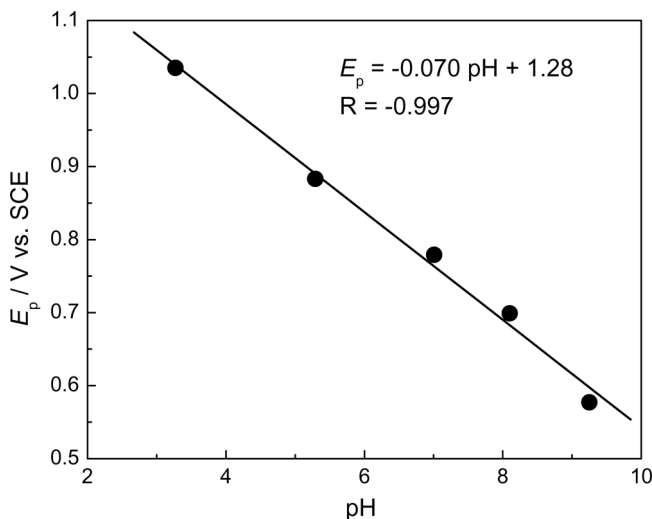
$E_p = -0.070 \text{ pH} + 1.28$
$R = -0.997$

Figure 3. Plot of peak potential E_p (●) vs. pH for the first oxidation peak from cyclic voltammograms of $7.0 \, \mu\text{mol} \, \text{L}^{-1}$ verapamil in buffer electrolyte.

$$I_{pa}(\mu\text{A}) = 0.12\nu^{1/2} + 0.12; \quad R = 0.999 \tag{4}$$

where the scan rate is in mV s^{-1}, showing diffusion-controlled mass transport. When $\log I_{pa}$ vs. $\log \nu$ is plotted, the slope of 0.42 confirms the diffusion-controlled mechanism (Brett and Oliveira Brett 1993).

Mechanism of Oxidation

These observations are in agreement with the mechanism proposed by Demircan, Kir, and Ozkan (2007), based on the findings of Bermejo et al. (2000), although in these studies a glassy carbon electrode was used. Demircan, Kir, and Ozkan (2007) also observed only one peak at low pH in cyclic voltammograms of solutions containing verapamil, whereas two peaks at greater pH values were observed, as in this work. Bermejo et al. (2000) noted similar phenomena when investigating mefexamide solutions—both verapamil and mefexamide contain methoxyphenyl and tertiary amine groups in their structures—and the sequence of peaks was attributed to the oxidation of the methoxyphenyl as a single peak at low pH and another peak at low potential at higher pH, attributed to oxidation of the tertiary amine.

To evaluate possible mechanisms, the electrochemical responses for the analyte in different buffers and in differential-pulse and square-wave voltammetry experiments were conducted under the conditions described in the experimental section. Square-wave voltammetric profiles showed only the forward current and no reverse current. In both cases, the peak width at half height was approximately $W_{1/2} \sim 120\,\mathrm{mV}$. As for cyclic voltammetry, the slope of the plot of E_p vs. pH was approximately $-0.060\,\mathrm{V}$. It was therefore deduced that both peaks correspond to irreversible processes involving one electron and one proton.

Characterization by Electrochemical Impedance Spectroscopy

The electrochemical behavior of this kind of sensor can be the result of interacting factors such as conductivity of the bulk electrode material and mass transport of electroactive substances toward the electrode and their reaction. The direct contact of neighboring conducting particles allows electrical conduction, which can be explained by percolation theory. However, the relaxation times are small compared with the timescale of electrochemical processes, so they can be considered perfect resistors (Beaunier et al. 2007). Thus, the form of the electrochemical impedance spectra reflects interfacial phenomena between the electrode and bulk solution.

For recording impedance spectra in pH 5.3 acetate buffer solution, applied potentials of $+0.6$, $+0.9$, and $+1.0\,\mathrm{V}$ vs. SCE were chosen, the first being a potential at which no electrochemical process of verapamil occurs and then other potentials related to the first oxidation peak of verapamil at $+0.9\,\mathrm{V}$ and the second at close to $+1.0\,\mathrm{V}$.

At $+0.6\,\mathrm{V}$, the spectra in electrolyte and in solutions containing verapamil showed no difference; on the other hand, at $+0.9\,\mathrm{V}$ (peak potential), a less resistive behavior of electrode in the presence of analyte was observed, returning to the initial one after the electrode was washed, which suggests that there was no permanent analyte adsorption, see Fig. 4. At $+1.0\,\mathrm{V}$, it can be seen that the presence of analyte led to irreversible changes to the surface, because after rinsing, the impedance spectrum did not return to the initial one (Fig. 4c).

These results suggest that the determination of the analyte under such conditions can be performed without surface renewal, making the procedure faster and easier than those with glassy carbon (Demircan, Kir, and Ozkan 2007).

The model used to analyze the spectra consisted of the cell resistance, R_1, in series with R_2 charge-transfer resistance in parallel with a constant-phase element (CPE), a typical equivalent circuit for composite electrodes; see Fig. 4d. Values for R_1 did not vary ($38\,\Omega \pm 0.5\%$), and the interfacial
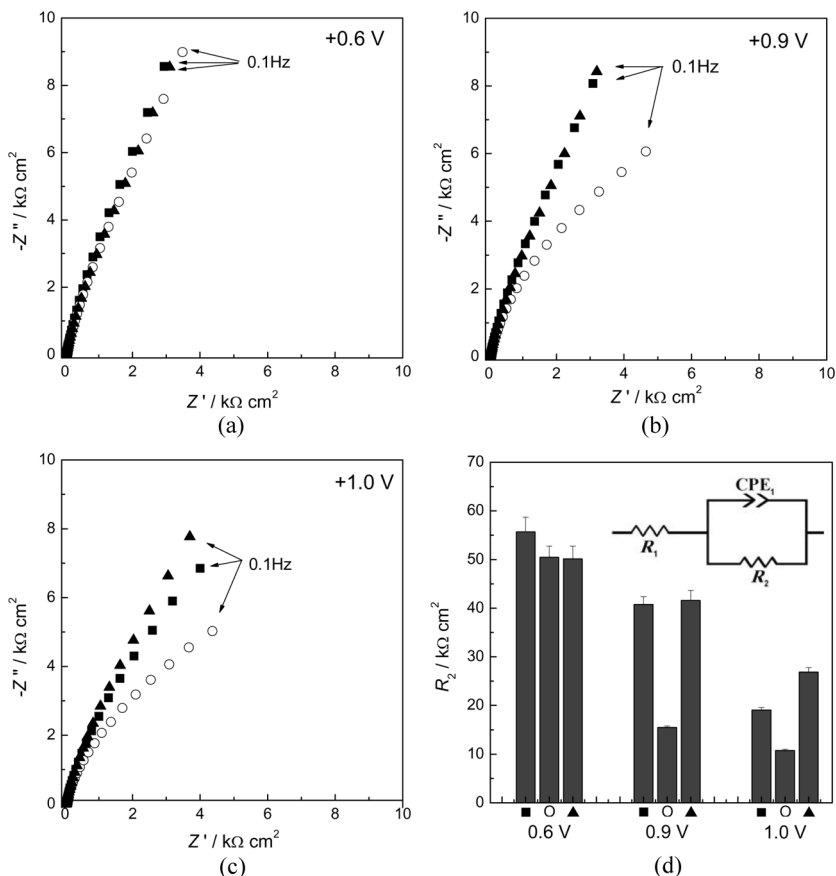
Figure 4. Complex plane impedance plots in pH 5.3 mol L^{-1} 0.1 M acetate buffer solution (■) without verapmil, (○) with 7×10^{-5} mol L^{-1} verapamil, and (▲) after rinsing at (a) +0.6 V, (b) +0.9 V, and (c) +1.0 V vs. SCE. (d) Values of R_2 deduced from fitting of the spectra to the circuit shown in the inset.

capacitance ($\sim$140 µF cm^{-2} s$^{-0.16}$) and CPE exponent α ($\sim$0.85) are in agreement with those previously reported for composites based on nonoriented graphite Beaunier et al. 2007. The resistance R_2 decreased in value in the presence of analyte oxidation, as would be expected (Fig. 4d).

Quantitative Determination and Analytical Parameters

The analysis of verapamil was carried out using cyclic, differential-pulse, and square-wave voltammetry up to a concentration of 300 µmol L^{-1}.
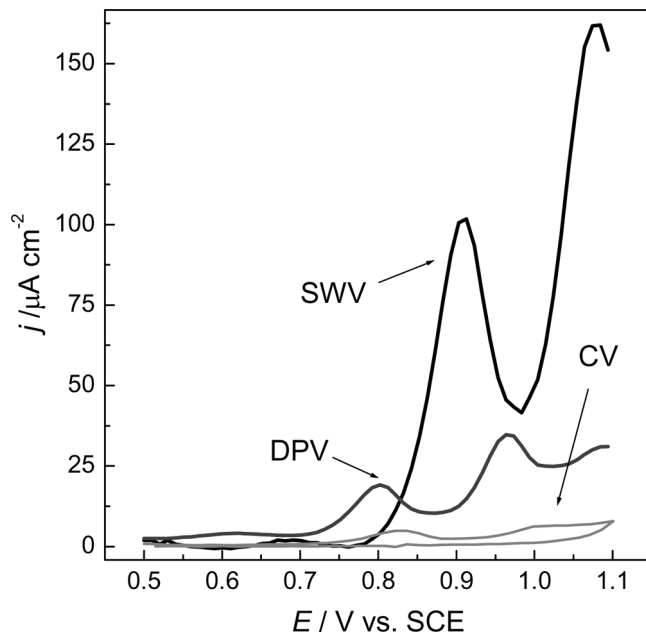
Figure 5. Electroanalysis of $6.6\,\mu mol\,L^{-1}$ verapamil in $0.1\,M$ acetate buffer solution, pH 5.3: Typical voltammetric profiles by cyclic voltammetry, differential-pulse voltammetry, and square-wave voltammetry using the optimized conditions described in the text.

Typical responses are shown in Fig. 5, and analytical parameters for all three techniques are collected in Table 3. The parameters obtained in this work are quite similar to those described by Demircan, Kir, and Ozkan (2007) for differential-pulse and square-wave voltammetry techniques at glassy carbon electrodes.

Table 3 Analytical parameters for quantification of verapamil: limit of detection (LoD), linear range (LR), and sensitivity

Technique	LoD ($\mu mol\,L^{-1}$)	LR ($\mu mol\,L^{-1}$)	Sensitivity ($L\,mol^{-1}\,cm^{-2}$)
Cyclic voltammetry	3.0	10–40	0.44
Differential-pulse voltammetry	0.7	2–30	2.00
Square-wave voltammetry	0.7	2–14	3.80

Cyclic Voltammetry

For quantitative determinations, the best results were obtained at a scan rate of $10\,mV\,s^{-1}$ using the second cycle. Peak currents were measured from cyclic voltammograms of verapamil solutions in different concentrations of the analyte in the range $3–295\,\mu mol\,L^{-1}$ taken at $10\,mV\,s^{-1}$ scan rate in pH 5.3 acetate buffer solution, resulting in a linear range from 10 to $40\,\mu mol\,L^{-1}$, with limits of detection and quantification of 3 and $10\,\mu mol\,L^{-1}$, respectively. A sensitivity of $0.44\,A\,L\,mol^{-1}\,cm^{-2}$ ($n = 7$, R = 0.9989) was found. The peak at more positive potentials was used because of its greater sensitivity.

Differential-Pulse Voltammetry

Quantification by differential-pulse voltammetry was carried out in pH 5.3 ($0.2\,mol\,L^{-1}$) acetate buffer supporting electrolyte. Experiments were carried out to assess the best pulse amplitude (10, 25, 50, and 100 mV) and scan rate (10, 25, 50, and $100\,mV\,s^{-1}$) from $+0.5$ to $+1.1\,V$ vs. SCE with $10\,\mu mol\,L^{-1}$ verapamil.

The better relationship between sensitivity and definition of peaks was reached using $100\,mV$ pulse amplitude and $25\,mV\,s^{-1}$ scan rate: two well-defined peaks were observed. Further studies investigated the relationship between peak potential and pH. Results suggested two independent peaks, each involving one electron per proton (slope close to $0.059\,V$ per pH unit and peak width at half height close to $120\,mV$).

The electrochemical response for the first peak was quantified in pH 5.3 solution using the optimized conditions in the range 0.3 to $50\,\mu mol\,L^{-1}$. The analytical parameters are shown in Table 3.

Square-Wave Voltammetry

The square-wave parameters of frequency (10, 25, 50, and 100 Hz), step (2, 5, and 10 mV), and square-wave amplitude (10, 25, and 50 mV) were optimized. The best conditions were a step potential of $10\,mV$ and amplitude of $50\,mV$ at 25 Hz. The sensitivity was approximately twice that obtained by differential-pulse voltammetry (see Table 3), the result of which was to reduce the linear range to $14\,\mu mol\,L^{-1}$ verapamil.

Analysis of Samples: Release Profiles

To evaluate the release profiles, aliquots taken from the commercial samples (after dissolution procedures and handling) were analyzed by
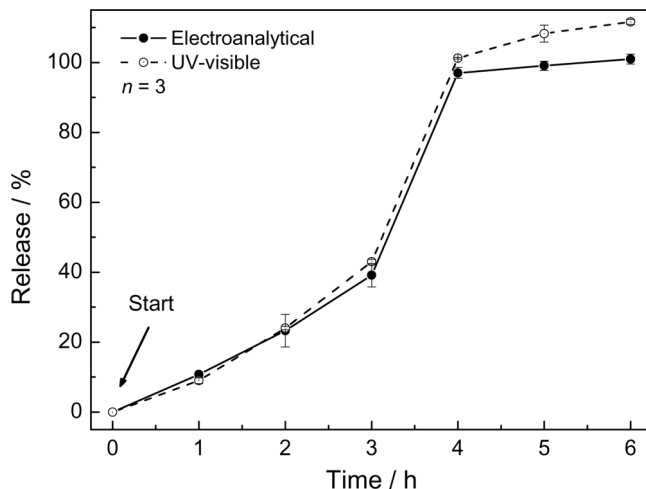
Figure 6. Release profiles for three samples of Dilacoron 120 mg Retard by differential-pulse voltammetry and spectrophotometric procedures.

cyclic, differential-pulse, and square-wave voltammetry and by UV-vis spectrophotometry for comparison.

Typical release profiles are shown in Fig. 6 for three commercial samples. Complete dissolution of the white-colored coating of the tablets occurred after approximately 3 h under the conditions reported in the experimental section, exposing the nucleus and thus increasing the rate of release of the active substance. The nuclei then dissolved, and complete release of verapamil was reached after 4 h. The presence of insoluble particles of excipients, such as magnesium stearate, did not interfere with the results. Good agreement between the electroanalytical and optical procedures was observed. The slightly greater spectrophotometric response for times longer than 4 h can be attributed to absorption of inert components of the nucleus, which began to be dissolved from then onward.

CONCLUSIONS

A solid graphite–polyurethane composite electrode without chemical modification has been used for the voltammetric quantification of verapamil in commercial samples without adsorption of the analyte or its oxidation products onto the electrode surface, demonstrating its viability for repetitive determinations without need of electrode surface

regeneration or renewal. The optimized procedures were applied to the determination of the release profiles of controlled-release tablets and compared to a spectrophotometric procedure.

This composite electrode is appropriate for use not only in batch procedures but also in flow or chromatographic systems because there are no complications from electrode surface adsorption phenomena.

REFERENCES

Aboukasim, E., Ghandour, M.A., El-Harty, M.T., and Ahmed, M.M. 2002. Determination of verapamil by adsorptive stripping voltammetry in urine and pharmaceutical formulations. *J. Pharm. Biomed. Anal.*, 30: 921–929.

Azarmi, S., Roa, W., and Löbenberg, R. 2007. Current perspectives in dissolution testing of conventional and novel dosage forms. *Int. J. Pharm.*, 328: 12–21.

Beaunier, L., Keddam, M., García-Jareño, J.J., Vicente, F., and Navarro–Boulais, J. 2007. Surface structure determination by SEM image processing and electrochemical impedance of graphite + polyethylene composite electrodes. *J. Electroanal. Chem.*, 566: 159–167.

Beevers, G., Lip, G., and O'Brien, E., eds. 2007. *ABC of Hypertension,* 5th ed. Oxford, UK: Blackwell.

Bermejo, E., Zapardiel, A., Pérez-López, J.A., Chicharro, M., Sánchez, A., and Hernández, L. 2000. Electrochemical study of mefexamide at glassy-carbon electrodes and its determination in urine by differential pulse voltammetry. *J. Electroanal. Chem.*, 481: 52–61.

Borges, N.C.C., Mendes, G.D., Barrientos-Astigarra, R.E., Gavinas, P., Oliveira, C.H., and Nucci, G. 2005. Verapamil quantification in human plasma by liquid chromatography coupled to tandem mass spectrometry: An application to bioequivalence study. *J. Chromatogr. B*, 827: 165–172.

Brett, C.M.A. and Oliveira Brett, A.M. 1993. *Electrochemistry: Principles, Methods, and Applications*. Oxford, UK: Oxford University Press.

Capella-Peiró, M.E., Font-Rubert, M., Alvarez-Rodríguez, L., Esteve-Romero, J., Durgbanshi, A., and Bose, D. 2007. Optimization using a factorial design for the separation of tandolapril and verapamil by capillary electrophoresis. *J. Liq. Chromatogr. Relat. Technol.*, 30: 2975–2988.

Cervini, P., Ramos, L.A., and Cavalheiro, E.T.G. 2007. Determination of atenolol at a graphite–polyurethane composite electrode. *Talanta*, 72: 206–209.

Demircan, S., Kir, S., and Ozkan, S.A. 2007. Electroanalytical characterization of verapamil and its voltammetric determination in pharmaceuticals and human serum. *Anal. Lett.*, 40: 1177–1195.

Donauer, N. and Löbenberg, R. 2007. A mini review of scientific and pharmaco-peial requirements for the disintegration test. *Int. J. Pharm.*, 345: 2–8.

Gil-Agustí, M., Carda-Broch, S., Capella-Peiró, M.E., and Esteve-Romero, J. 2006. Micellar liquid chromatographic determination of five antianginals in pharmaceutics. *J. Pharm. Biomed. Anal.*, 41: 1235–1242.

Hassan, S.S.M., Mahmoud, W.H., Elmosallamy, M.A.F., and Abdel-Samad, M.S. 1999. Miniaturized verapamil solid-state potentiometric sensors based on native ionic polymers. *Mikrochim. Acta*, 131: 199–203.

Hsieh, D.S., ed. 1993. *Drug Permeation Enhancement: Theory and Applications*. Drugs and the Pharmaceutical Sciences, vol. 62. New York: Informa HealthCare.

Jhee, O.H., Hong, J.W., Om, A.S., Lee, M.H., Lee, W.S., Shaw, L.M., Lee, J.W., and Kang, J.S. 2005. Direct determination of verapamil in rat plasma by coupled column microbore-HPLC method. *J. Pharm. Biomed. Anal.*, 37: 405–410.

Karsa, D.R. and Stephenson, R.A. eds. 1994. *Excipients and Delivery Systems for Pharmaceutical Formulations*. Cambridge, UK: Royal Society of Chemistry.

Kristoffersen, L., Oiestad, E.L., Opdal, M.S., Krogh, M., Lundanes, E., and Christophersen, A.S. 2007. Simultaneous determination of six beta-blockers, three calcium-channel antagonists, four angiotensin-II antagonists, and one antiarrhythmic drug in post-mortem whole blood by automated solid phase extraction and liquid chromatography mass spectrometry: Method development and robustness testing by experimental design. *J. Chromatogr. B*, 850: 147–160.

Li, S., Liu, G., Jia, J., Liu, Y., Pan, C., Yu, C., Cai, Y., and Ren, J. 2007. Simultaneous determination of 10 antiarrhythmic drugs and a metabolite in human plasma by liquid chromatography–tandem mass spectrometry. *J. Chromatogr. B*, 847: 174–181.

Marvola, M., Kannikoski, A., Aito, H., and Nykänen, S. 1991. *Pharmaceutical Technology: Controlled Drug Release*, ed. J. I. Wells, vol. 2. Chichester, UK: Ellis Horwood.

Mendes, R.K., Cervini, P., and Cavalheiro, E.T.G. 2006. The use of a graphite–castor oil polyurethane composite electrode for the determination of hydroquinone in photographic developers. *Talanta*, 68: 708–712.

Mendes, R.K., Claro-Neto, S., and Cavalheiro, E.T.G. 2002. Evaluation of a new rigid carbon–castor oil polyurethane composite as an electrode material. *Talanta*, 57: 909–917.

Moser, M. 2008. *Clinical Management of Hypertension*, 8th ed. West Islip, NY: Professional Communications.

Ortuño, J.A., Hernández, J., and Sánchez-Pedreño, C. 2006. Ion-selective electrode for the determination of some multidrug resistance reversers. *Sens. Actuators B*, 119: 282–287.

Ortuño, J.A., Sánchez-Pedreño, C., and Gil, A. 2005. Flow injection pulse amperometric detection based on ion transfer across a water-plasticized polymer membrane interface for the determination of verapamil. *Anal. Chim. Acta*, 554: 172–176.

Patlak, M. 2003. From viper's venom to drug design: Treating hypertension: Breakthroughs in biosciences. *FASEB J.*, 18: 421.

Rahman, N. and Azmi, S.N.H. 2004. Spectrophotometric method for the determination of verapamil hydrochloride in pharmaceutical formulations using N-bromosuccinimide as oxidant. *Farmaco*, 59: 529–536.

Rahman, N. and Hoda, M.D.N. 2002. Spectrophotometric determination of verapamil hydrochloride in drug formulations with chloramine-T as oxidant. *Anal. Bioanal. Chem.*, 374: 484–489.

Rambla-Alegre, M., Gil-Agustí, M.T., Capella-Peiró, M.E., Carda-Broch, S., and Esteve-Romero, J.S. 2005. Direct determination of verapamil in urine and serum samples by micellar liquid chromatography and fluorescence detection. *J. Chromatogr. B*, 839: 89–94.

Ramírez-Campos, M. and Villafuerte-Robles, L. 2004. Effect of formulation variables on verapamil hydrochloride release from hydrated HPMC matrices. *Rev. Soc. Quím. México*, 48: 326–331.

Silva, J.C.G.E., Leitão, J.M.M., Costa, F.S., and Ribeiro, J.L.A. 2002. Detection of verapamil drug by fluorescence and trilinear decomposition techniques. *Anal. Chim. Acta*, 453: 105–115.

Teixeira, M.F.S., Marcolino-Júnior, L.H., Fatibello-Filho, O., Dockal, E.R., and Bergamini, M.F. 2007. An electrochemical sensor for L-DOPA based on oxovanadium–salen thin film electrode applied flow injection system. *Sens. Actuators B*, 122: 549–555.

Toledo, R.A., Santos, M.C., Cavalheiro, E.T.G., and Mazo, L.H. 2005. Determination of dopamine in synthetic cerebrospinal fluid by SWV with a graphite–polyurethane composite electrode. *Anal. Bioanal. Chem.*, 381: 1161–1166.

Toledo, R.A., Santos, M.C., Honório, K.M., Silva, A.B.F., Cavalheiro, E.T.G., and Mazo, L.H. 2006. Use of graphite–polyurethane composite electrode for imipramine oxidation: Mechanism proposal and electroanalytical determination. *Anal. Lett.*, 39: 507–520.

Toledo, R.A. and Vaz, C.M.P. 2007. Use of a graphite–polyurethane composite electrode for electroanalytical determination of índole-3-acetic acid in soil samples. *Microchem. J.*, 86: 161–165.

Venkatesh, G., Ramanathan, S., Mansor, S.M., Nair, N.K., Sattar, M.A., Croft, S.L., and Navaratnam, V. 2007. Development and validation of RP-HPLC-UV method for simultaneous determination of buparvaquone, atenolol, propranolol, quinidine, and verapamil: A tool for the standardization of rat in situ intestinal permeability studies. *J. Pharm. Biomed. Anal.*, 43: 1546–1551.

Von Stackelberg, M., Pilgram, M., and Toome, V. 1953. Bestimmung von Diffusionkoeffizienten einiger Ionen in wäßriger Lösung in Gegenwart von Fremdelektrolyten. *Z. Elektrochem.*, 57: 342–350.

Walles, M., Mullett, W.M., Levsen, K., Borlak, J., Wunsch, G., and Pawliszyn, J. 2002. Verapamil drug metabolism studies by automated in-tube solid phase microextraction. *J. Pharm. Biomed. Anal.*, 30: 307–319.

Xu, D., Liu, S., Liu, Z., and Hu, X. 2007. Determination of verapamil hydrochloride with 12-tungstophosphoric acid by resonance Rayleigh scattering method coupled to flow injection system. *Anal. Chim. Acta*, 588: 10–15.